GROWTH AND RAMAN SCATTERING CHARACTERIZATION OF Cu_2ZnSnS_4 THIN FILMS

P.A. Fernandes[1,2], P.M.P. Salomé[1], A.F. da Cunha[1]

[1]Departamento de Física, Universidade de Aveiro, Campus Universitário de Santiago, 3810-193 Aveiro, Portugal

[2]Departamento de Física, Instituto Superior de Engenharia do Porto, Instituto Politécnico do Porto, Rua Dr. António Bernardino de Almeida, 431, 4200-072 Porto, Portugal

Abstract:

In the present work we report the results of the growth, morphological and structural characterization of Cu_2ZnSnS_4 (CZTS) thin films prepared by sulfurization of DC magnetron sputtered Cu/Zn/Sn precursor layers. The adjustment of the thicknesses and the properties of the precursors were used to control the final composition of the films. Its properties were studied by SEM/EDS, XRD and Raman scattering. The influence of the sulfurization temperature on the morphology, composition and structure of the films has been studied. With the presented method we have been able to prepare CZTS thin films with a kesterite structure.

Keywords: Cu_2ZnSnS_4, CZTS, sputtering, sulfurization, thin film, solar cell, Raman

1. Introduction

Nowadays best thin film solar cells maximum efficiencies are approaching mono-crystalline Si-based ones [1]. Despite that, these still use rare and expensive materials like In, Ga and Te, they also use toxic elements like Cd and Se, which represent a disadvantage. Cu_2ZnSnS_4 (CZTS) can be a good choice for a new absorber layer presenting an absorption coefficient over 10^4 cm^{-1} and a band-gap energy near 1.45 eV [2]. Several procedures have already been studied for the growth of CZTS. Thermal evaporation was tested by T. Friedlmeier *et al.* [3]. E-Beam evaporation with a post

sulfurization process was studied by Takagiri *et al.* [4]. K. Jimbo *et al.* were successful in growing CZTS using RF co-sputtering of binary compounds [5]. Routes using co-evaporated elements were developed by T. Tanaka *et al.* [6]. So far the highest efficiency reported for CZTS solar cells is 5.7% and it was achieved by K. Jimbo *et al.* [5]. Non vacuum methods have also been developed, namely sulfurization of sol-gel deposited precursors by K. Tanaka *et al.* and spray-pyrolysis by N. Nakayama *et al.* and N. Kamoun *et al.* [7 - 9].

In this work we study a two step method to grow CZTS. This method uses a sequential deposition of metallic precursors by DC magnetron sputtering on soda lime glass (SLG) coated with Mo. These layers are then heated up in a Sulphur (S) + Nitrogen gas (N_2) atmosphere.

2. Experimental Details

2.1. Sample Preparation

The method used in this work can be divided in two stages. First, a sequential deposition of the metallic precursor layers is performed by DC magnetron sputtering. The second stage is the formation of the CZTS layer by sulfurization of the precursors.

The sample preparation process begins with the substrate cleaning, a 9 cm^2 SLG, with successive ultrasound baths of acetone/alcohol/deionised water. This step ends with substrate being dried with a N_2 flow. The back contact layer is a Mo bilayer deposited by DC magnetron sputtering (target purity 99.95%). The deposition conditions followed the recipe developed by J. Scofield *et al.* to ensure both low resistivity and good adhesion to the SLG [10]. A sequential deposition of metallic precursors was performed using an Ar atmosphere and an operating pressure of 2×10^{-3} mbar. The deposition order was Cu (target purity 99.999%), Zn (target purity 99.99%) and finally Sn (target purity 99.99%). Several deposition power settings were used with the following values 0.16 Wcm^{-2},

0.16-0.38 Wcm^{-2}, 0.11-0.16 Wcm^{-2} for Cu, Zn and Sn, respectively. The individual thicknesses were estimated using the density and molecular weight of each element. *In situ* monitoring of the layer thicknesses was done with a quartz crystal monitor.

For the second stage, which refers to CZTS formation, a temperature controlled tubular furnace, was used. The sample was heated in a N_2 atmosphere at an operating pressure of 5.6×10^{-1} mbar. The sample heating rate was 10 ºC/min. The sulfurization temperature profile, for a maximum temperature of 525 ºC, is sketched in figure 1. In this stage the only parameter changed, between samples, was the maximum sulfurization temperature. The Sulphur evaporation source was a quartz tube filled with elemental Sulphur pellets (purity 99.999%). The evaporation temperature was 130 ºC and the N_2 flow rate was 40 ml/min.

2.2. Characterization

Confirmation of individual metallic precursor layer and CZTS thicknesses was done using stylus profilometry technique with a Veeco Dektak 150 surface profiler. The structural analysis of the CZTS thin films was done by X-ray diffraction on a PHILIPS PW 3710 device equipped with a Cu-Kα source (wavelength λ=1.54060 Å) and the generator settings were 50 mA, 40 kV. The SEM/EDS systems used were a SEM Hitachi S4100 and a Rontec EDS with setting parameters of 25 KeV and 10 μA for surface imaging and a Hitachi SU-70 with a Quantax Bruker AXS EDS system with 15/25 KeV and 40 μA for cross-section imaging. For Raman spectroscopy, the LASER line used was 514.5 nm and the device was a Jobin-Yvon T64000.

3. Results and Discussion

Since there is a lack of information on the thermodynamics of CZTS thin film formation, the initial study was aimed at clarifying this issue. The second study was a detailed analysis of the best CZTS samples.

In this approach all the metallic precursor thicknesses were kept constant with the following values, Cu-150 nm, Zn-190 nm and Sn-340 nm. The sulfurization temperatures were 330 ºC, 370 ºC, 425 ºC and 505 ºC. This parameter was used to name the various samples. The EDS analysis showed that all samples had an excess of Sn and an average concentration ratio of 0.87 and 0.40 for [Cu]/([Zn]+[Sn]) and [Zn]/[Sn], respectively. The results of Raman scattering and XRD analysis are presented in figure 2 and figure 3, respectively. For the sample S330, the Raman spectra shows evidence of the presence of SnS with characteristic modes at 160 cm^{-1}, 190 cm^{-1}, 220 cm^{-1} and SnS_2 with a mode at 315 cm^{-1} this assignment of the peaks is in agreement with data reported by other authors [11]. XRD analysis confirmed the presence of the binary compounds. The Raman analysis for sample S370 only shows the existence of SnS_2 peak at 315 cm^{-1}. Again XRD data provides a confirmation of the presence of SnS_2. In both samples, XRD analysis detected elemental Zn. For S425 the Raman scattering analysis shows major peaks, at 264 cm^{-1}, 304 cm^{-1} and 356 cm^{-1} corresponding to $Cu_{2-x}S$ [12], Sn_2S_3 [11] and cubic ZnS [13], respectively. This sample's XRD pattern matches the peaks of β-ZnS according to [14]. Note that the spectra of CZTS and β-ZnS are very similar for visible peaks and the angle differences are within the instrument accuracy. There can be also some stress-related shifts that might cause changes of this magnitude. These facts turn the XRD identification of CZTS a difficult task. For sample S505, the Raman characterization shows a single peak at 338 cm^{-1}. XRD analysis shows both ZnS and CZTS to be present. Since there is almost no cubic ZnS Raman peak and the only published data of Raman is for monograins not for thin films we have associated the 338cm^{-1} peak to CZTS [15]. This fact reveals the importance of Raman analysis to distinguish between β-ZnS and CZTS.

Using the results just discussed we have increased the sulfurization temperature to 525 ºC and corrected the chemical composition of the precursors. EDS analysis was used to determine chemical composition of metallic precursors and CZTS. The element concentration ratio is shown in table 1. From this table it can be observed that the sulfurization process causes a loss in Zn concentration. Although it is not observed in these results, a small loss of Sn also occurs in most cases. It can be explained by evaporation of these two elements during the heating process under vacuum.

From the XRD pattern, figure 4, it can be observed the presence of CZTS with a preferential growth orientation of (112). The sharpness of the major peaks indicates a good crystallinity. These results have also confirmed the presence of binary chalcogenides, such as sphalerite ZnS and covellite $Cu_{2-x}S$. The figure 5 shows the results of Raman scattering in two zones of the sample S525. The existence of CZTS is confirmed by the presence of Raman peaks at 338-339 cm^{-1}, 288 cm^{-1} and 256-257 cm^{-1}. These are in agreement with the published data for monograins of CZTS [15]. Zone 1 show a strong peak for $Cu_{2-x}S$ at 476 cm^{-1} which is not observed in zone 2 [12]. The spectra of both zones exhibit a shoulder at 255 cm^{-1}, which is believed to be the convolution of peaks corresponding to Sn_2S_3, CZTS, $Cu_{2-x}S$ and ZnS [11-15]. ZnS is also detected with Raman analysis with peaks located at 348 cm^{-1} [13].

The morphology and grain size was analysed using a SEM and the results are presented in figure 6 and 7. Figure 6 shows good crystallinity and compactness of the CZTS layer. The surface shows some roughness and few voids. Figure 7 shows sparse large grains that have been identified as $Cu_{2-x}S$ crystallites. Their composition was confirmed with EDS analysis. Figure 8 shows the cross section SEM image of the S525 with layer thickness indication. It shows that the CZTS layer has a thickness of 1.5 µm. It can be observed a void or cavity between the CZTS and the Mo layer which

could be created either during the film growth or during the cutting process. Nevertheless, these pictures show a compact CZTS layer and confirm the presence of $Cu_{2-x}S$ situated at the top of the film.

4. Conclusions

This work shows that it is possible to grow the Cu_2ZnSnS_4 absorber layer with this two-step procedure. Further research must be carried out to optimize the film quality, to produce a more compact layer and to improve the adhesion of the absorber layer to the back-contact. The elimination of $Cu_{2-x}S$ phases may be performed using a more accurate composition control of the metallic precursors and/or a chemical surface treatment with KCN.

It was also proved that, since in XRD analysis it is difficult to distinguish between ZnS and CZTS, Raman analysis is an important and a complementary analysis method. The thin film CZTS Raman modes appear at the same wavenumbers as those of monograin CZTS.

5. Bibliography:

[1] Ingrid Repins, M. Contreras, B. Egaas, C.DeHart, J. Scharf, C.Perkins, B. To and R. Noufi, Prog. in Photovolt.: Research and Applications, Volume 16, Issue 3 , Pages 235 – 239.

[2] J.M. Raulot, C. Domain , J.F. Guillemoles, Journal of Physics and Chemistry of Solids 66 (2005) 2019–2023.

[3] Th. Friedlmeier, N. Wieser, Th. Walter, H. Dittrich, H.-W. Schock, Proceedings of the 14th European PVSEC and Exhibition, 1997, P4B.10.

[4] H. Katagiri, K. Saitoh, T. Washio, H. Shinohara, T. Kurumadani, S. Miyajima, Solar Energy Materials and Solar Cells, Volume 65, Issues 1-4, January 2001, Pages 141-148.

[5] KK. Jimbo, R. Kimura, T. Kamimura, S. Yamada, W. Maw, H. Araki, K. Oishi, H. Katagiri, Thin Solid Films, Volume 515, Issue 15, 31 May 2007, Pages 5997-5999.

[6] T. Tanaka, D. Kawasaki, M. Nishio, Q. Guo, H. Ogawa, Phys. Stat. sol. (c) 3, No. 8, 2844-2847 (2006).

[7] K. Tanaka, N. Moritake, H. Uchiki, Solar Energy Materials and Solar Cells, Volume 91, Issue 13, 15 August 2007, Pages 1199-1201.

[8] N. Nakayama and K. Ito, Applied Surface Science, vol. 92, pp. 171-175, 1996.

[9] N. Kamoun, H. Bouzouita, B. Rezig, Thin Solid Films, Volume 515, Issue 15, 31 May 2007, Pages 5949-5952.

[10] John H. Scofield, A. Duda, D. Albin, B. L. Ballard, P. K. Predecki, *Thin Solid Films*, *Volume 260, Issue 1*, *1 May 1995*, *Pages 26-31.*

[11] I. P. Parkin, L. S. Price, T. G. Hibbertb and K. C. Molloyb, J. Mater. Chem., 2001, 11, 1486–1490.

[12] Carolyn G. Muncea, Gretel K. Parker a, Stephen A. Holt b, Gregory A. Hopea, Colloids and Surfaces A: Physicochem. Eng. Aspects 295 (2007) 152–158.

[13] J. Serrano, A. Cantarero, M. Cardona, N. Garro, R. Lauck, R. E. Tallman, T. M. Ritter and B. A. Weinstein, PHYSICAL REVIEW B 69, 014301, 2004.

[14] International Centre for Diffraction Data, 14 04-005-0388 (CZTS), 04-004-3804 (Cubic ZnS), 04-004-3831 (Orthorhombic-Sns), 04-003-4154 (Hexagonal - SnS2), 04-001-1461 (Hexagonal – CuS).

[15] M. Altosaar, J. Raudoja, K. Timmo, M. Danilson, M. Grossberg, J. Krustok, and E. Mellikov, p hys. stat. sol. (a) 205, No. 1, 167–170 (2008)

Precursor metallic layers (before sulfurization)		CZTS (after sulfurization)		
Composition ratio		Composition ratio		
[Cu]/([Zn]+[Sn])	[Zn]/[Sn]	[Cu]/([Zn]+[Sn])	[Zn]/[Sn]	Metal/S
0.87	1.09	0.90	0.87	1.03

Table 1: Composition ratios for metallic precursor layers and CZTS.

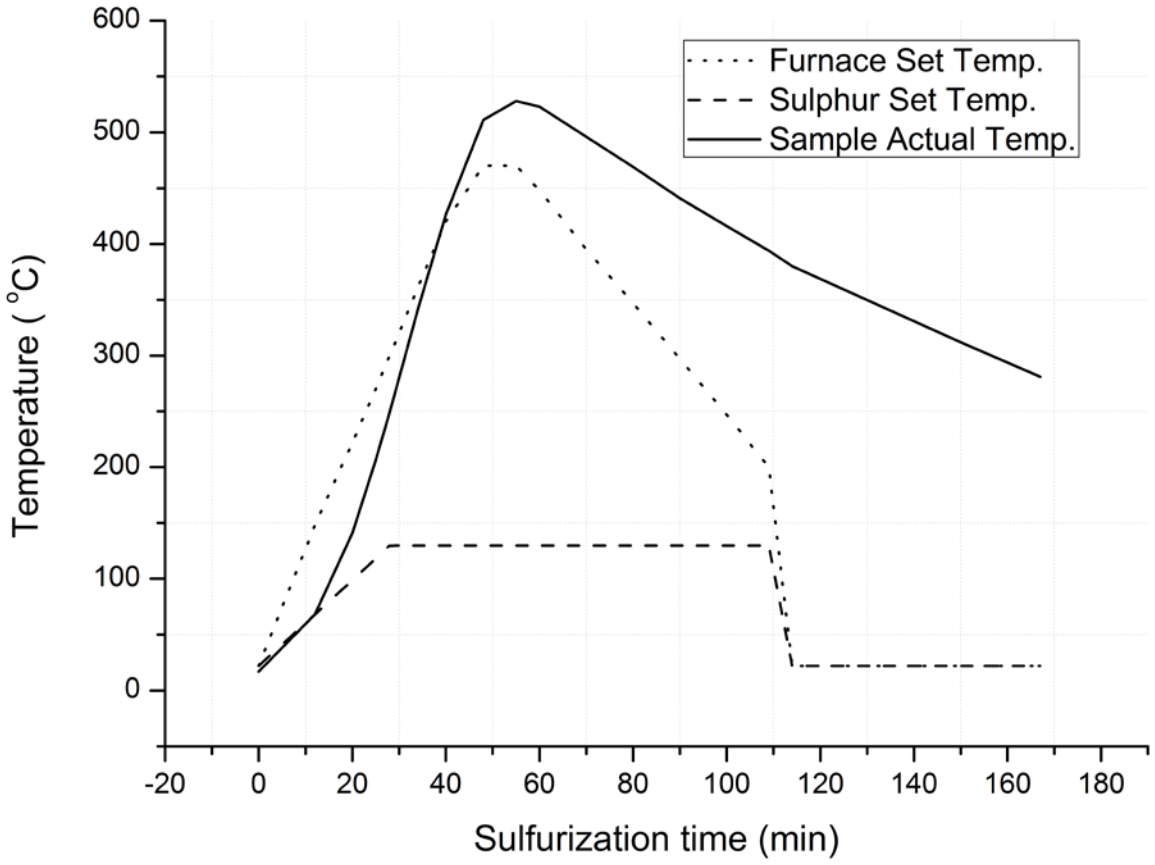

Figure 1: Furnace, sample and Sulphur source temperature profiles.

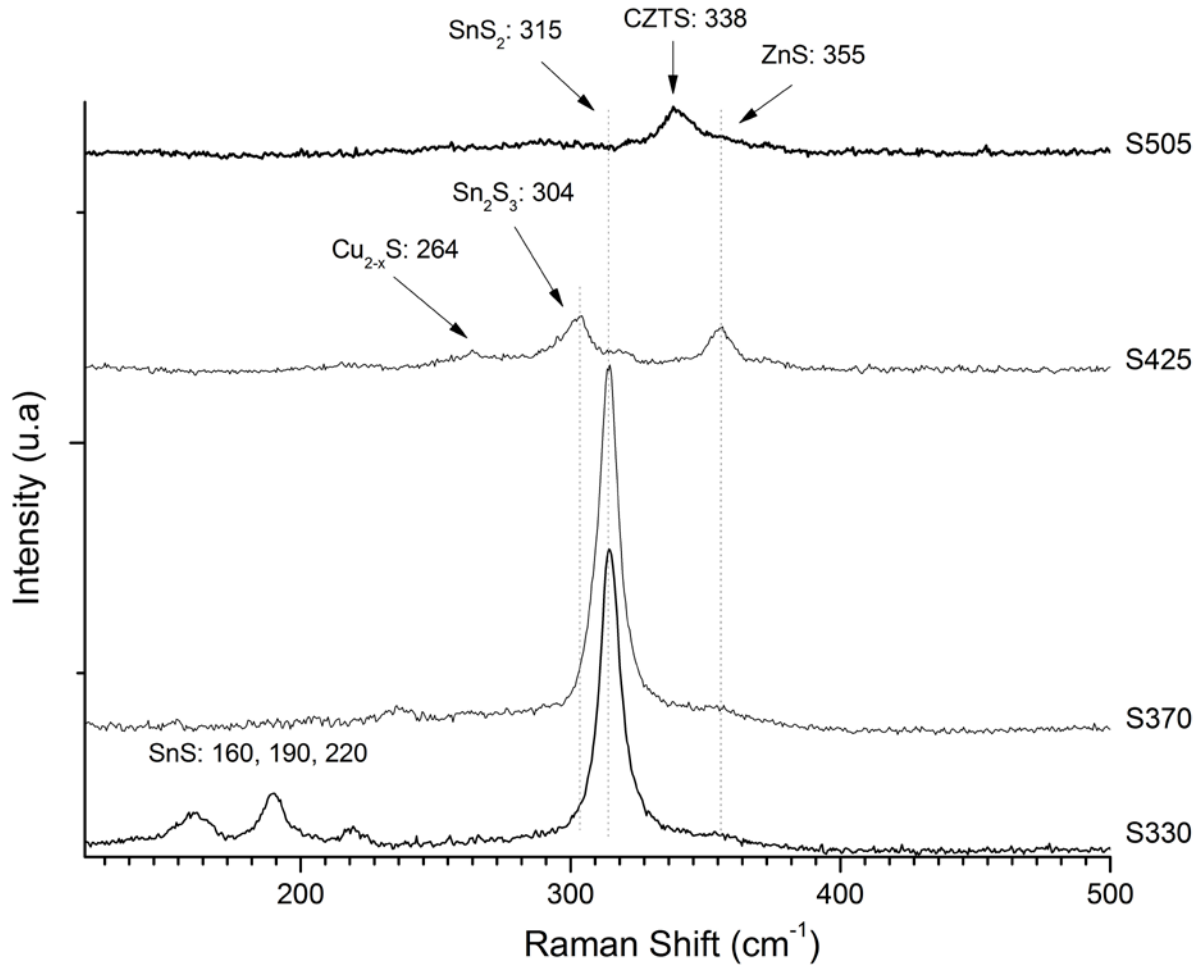

Figure 2: Raman scattering results for various sulfurization temperatures. Major peak assignment is performed using the following references: tin sulphides [11], copper sulphides [12], zinc-blende zinc sulphides [13] and CZTS [15] and XRD analysis.

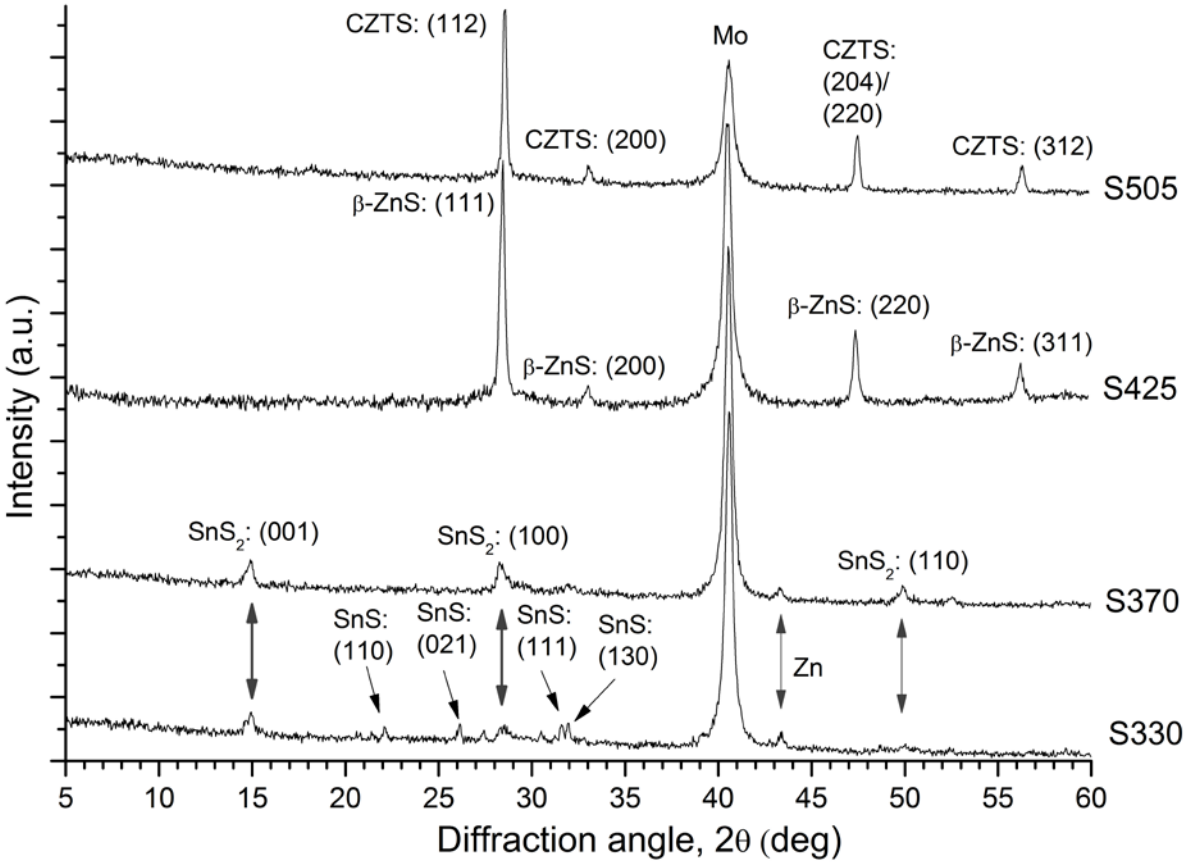

Figure 3: XRD pattern for various sulfurization temperatures. Major peak identification is made using data reported in reference [14] combined with Raman analysis.

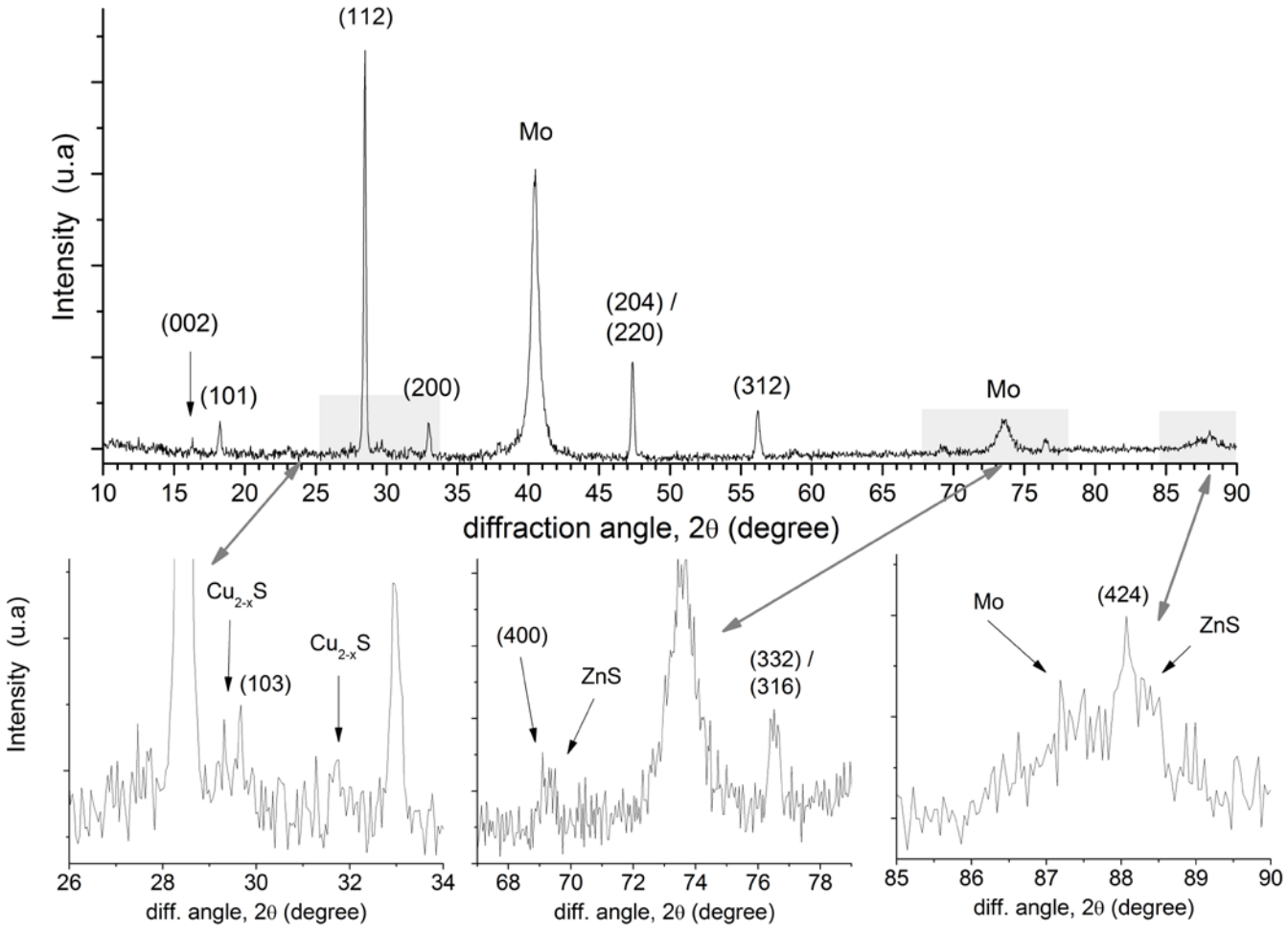

Figure 4: XRD spectrum of S525. Orientation planes are presented for CZTS using reference [14]. Detailed graphs show traces of $Cu_{2-x}S$ and ZnS phases [14].

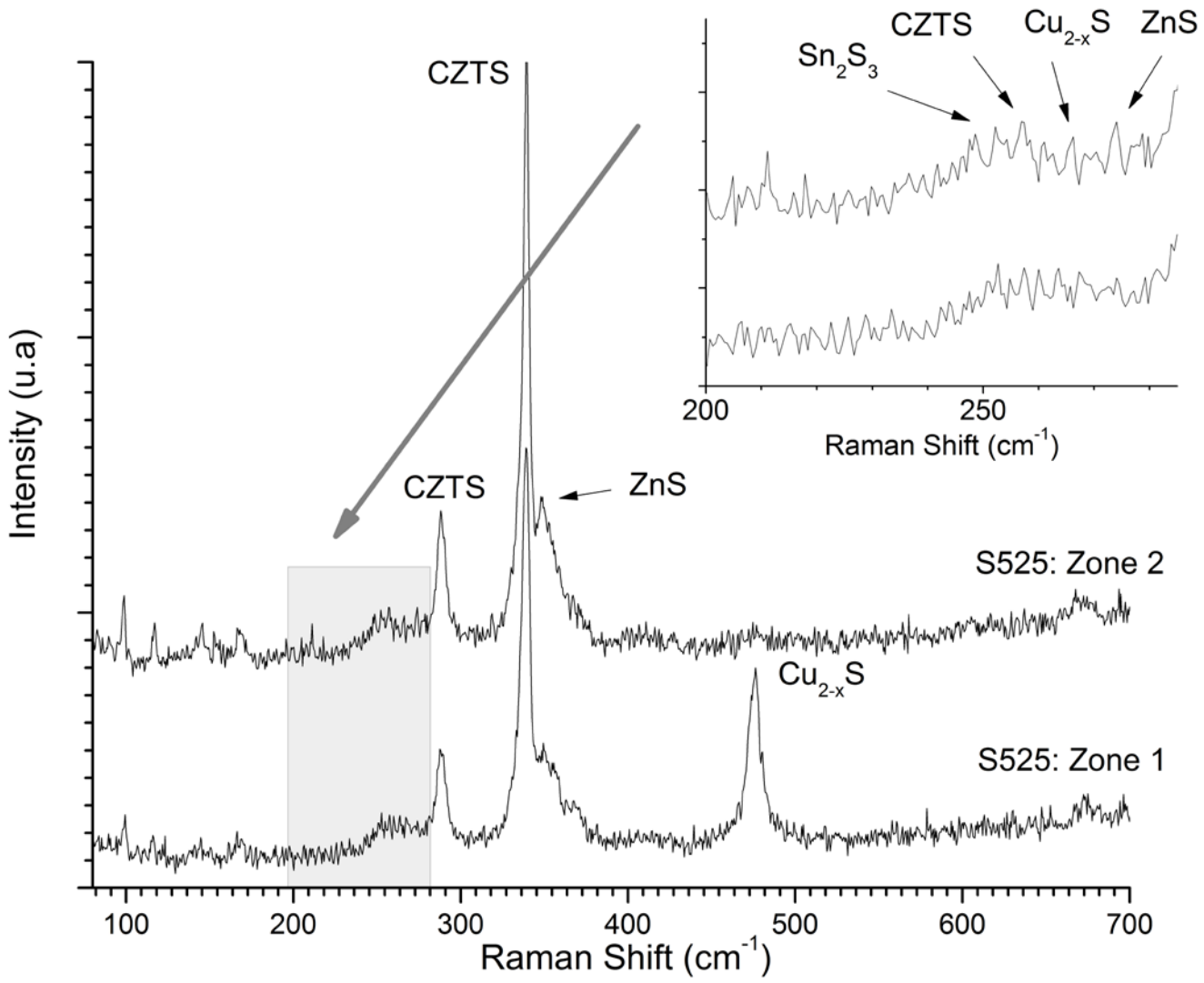

Figure 5: Raman analysis of sample S525 in 2 different zones. The main difference between these two results is the $Cu_{2-x}S$ peak at 475 cm^{-1}. The three major CZTS peaks are detected at 339 cm^{-1}, 288 cm^{-1} and 257 cm^{-1} [15]. The cubic structured ZnS is shown at 350 cm^{-1} and at 274 cm^{-1} (zoomed graphs) [13]. Detailed graphs also indicate traces of other sulphide compounds [11-12].

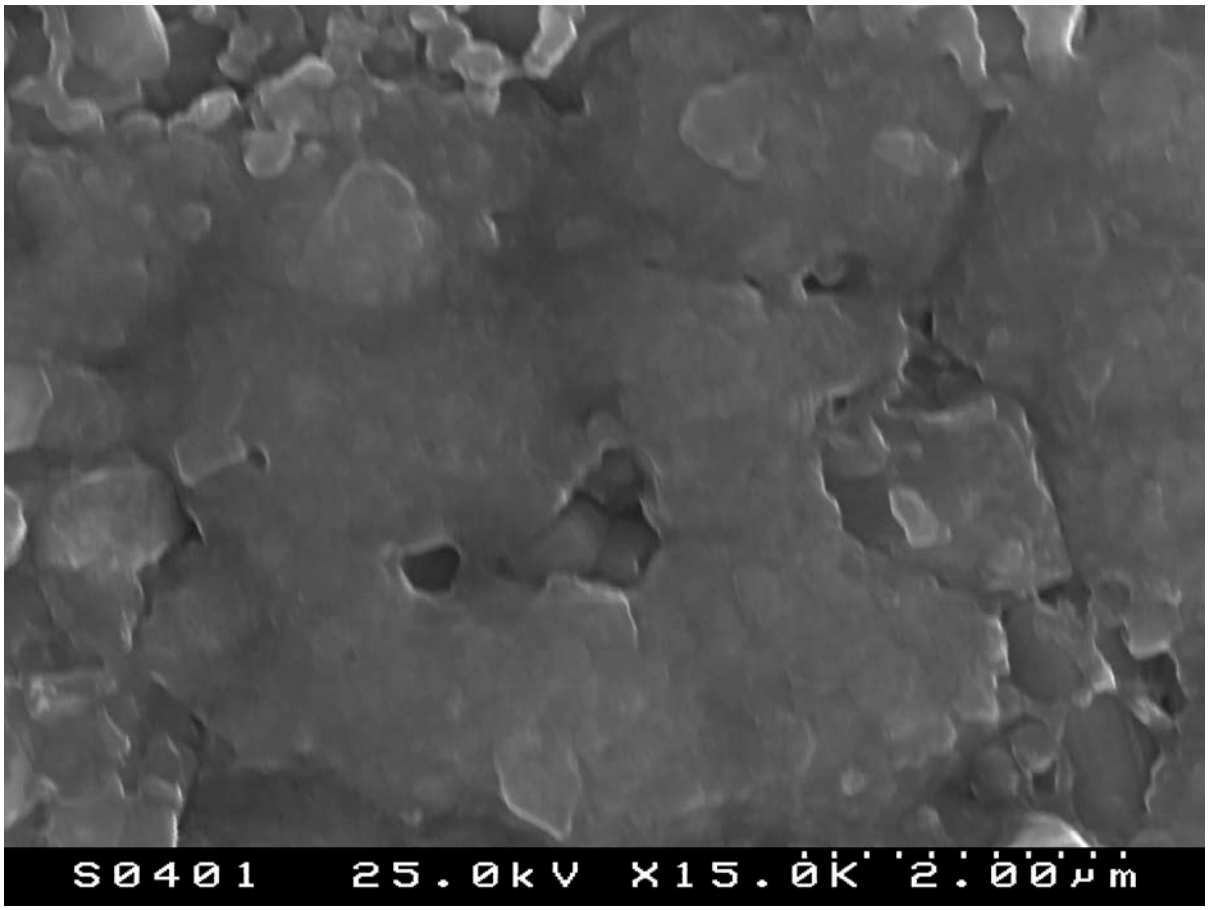

Figure 6: SEM micrograph of the CZTS surface. Despite presenting a compact film this sample presents some holes and some roughness.

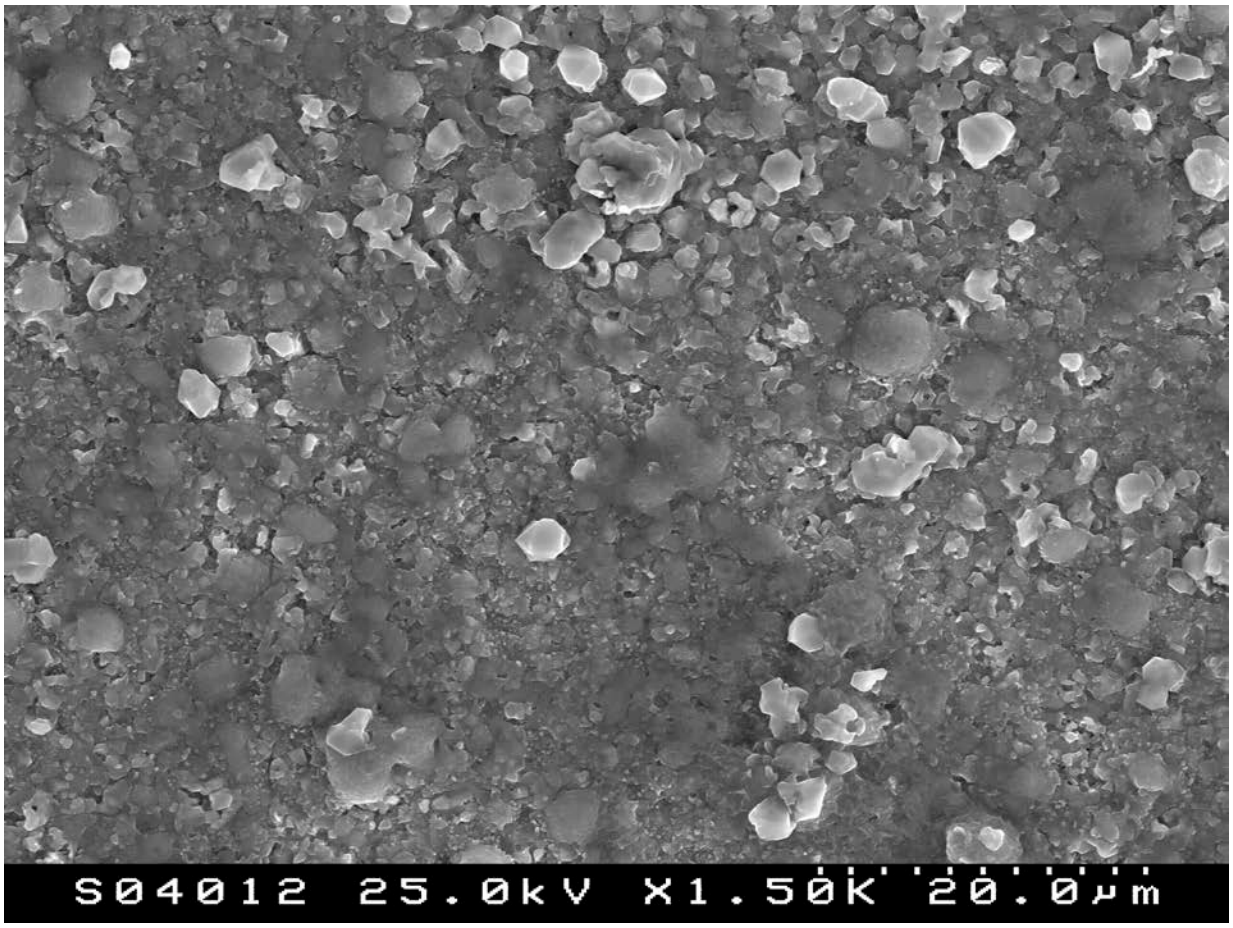

Figure 7: SEM micrograph of the CZTS surface. Some $Cu_{2-x}S$ crystallites are visible.

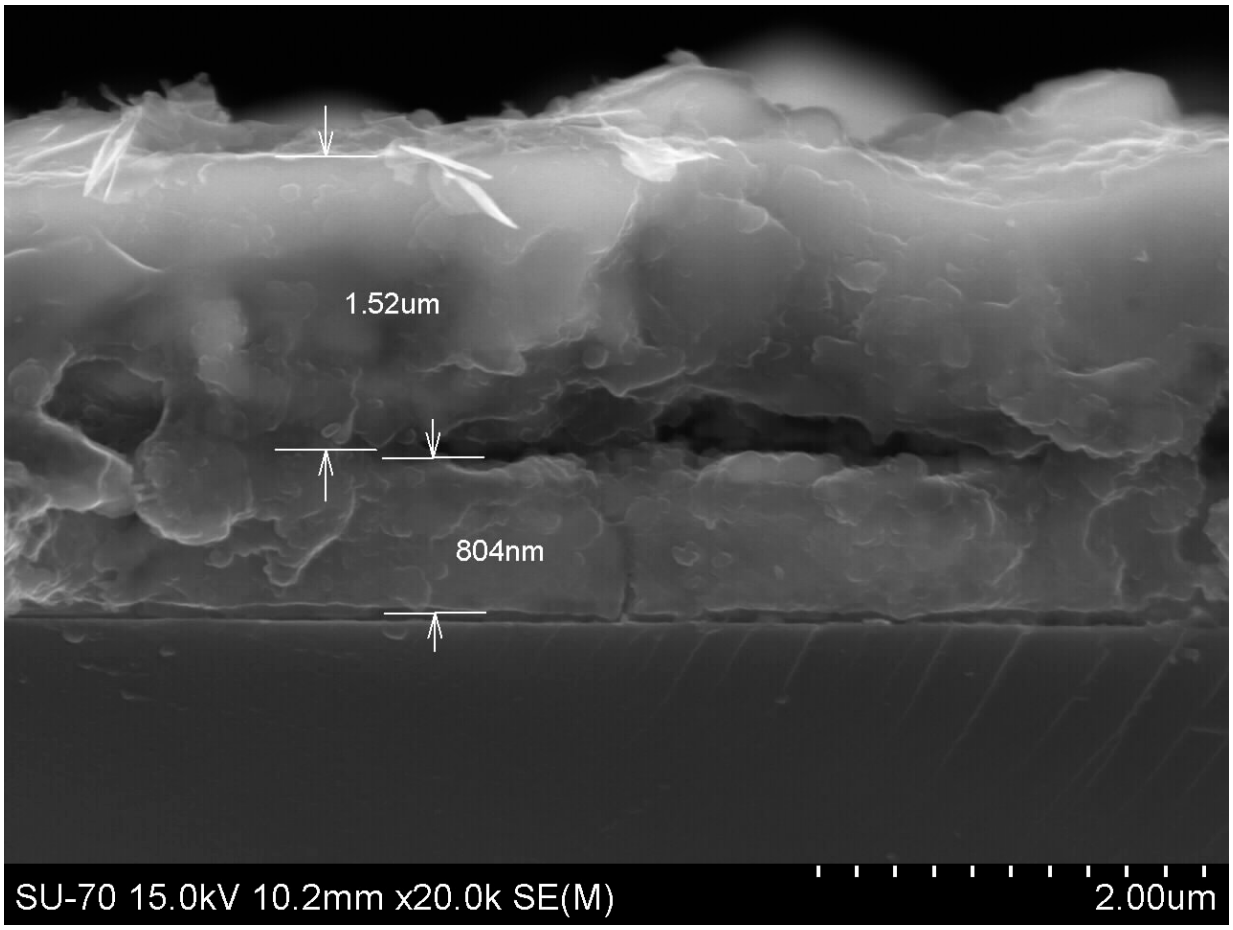

Figure 8: SEM micrograph of the CZTS and Mo cross-section. The thicknesses are close to 1.5 μm and 800 nm for CZTS and Mo, respectively.